Article:
Allocca, G., Kusumbe, A.P., Ramasamy, S.K. et al. (2016) Confocal/two-photon microscopy in studying colonisation of cancer cells in bone using xenograft mouse models. BoneKEy Reports, 5.

https://doi.org/10.1038/bonekey.2016.84

Title: Confocal/two-photon microscopy in studying colonisation of cancer cells in bone using xenograft mouse models

Gloria Allocca[1], Anjali P. Kusumbe[2], Saravana K. Ramasamy[3,4], Ning Wang[1*]

Affiliations:

[1] The Mellanby Centre for Bone Research, Department of Oncology and Metabolism, The University of Sheffield, Sheffield S10 2RX, UK

[2] Kennedy Institute of Rheumatology, University of Oxford, Roosevelt Drive, Headington, Oxford OX3 7FY, UK

[3] Integrative Skeletal Physiology group, Institute of Clinical Sciences, Imperial College London, London, W12 0NN, UK

[4] MRC Clinical Sciences Centre, Du Cane Road, London, W12 0NN, UK

*Corresponding author and address for reprint requests:

Dr Ning Wang

The Mellanby Centre for Bone Research

Department of Oncology and Metabolism

The University of Sheffield

Beech Hill Road, Sheffield, S10 2RX

UK

Phone: (+44) 0114 2159216

Fax: (+44) 0114 271 2475

Running title: Confocal/two-photon in bone oncology research

Abstract

Confocal and two-photon microscopy has been widely used in bone research to not only produce high quality, three-dimensional (3D) images but also to provide valuable structural and quantitative information. In this article, we describe step-by-step protocols for confocal and two-photon microscopy to investigate earlier cellular events during colonisation of cancer cells in bone using xenograft mouse models. This includes confocal/two-photon microscopy imaging of paraformaldehyde (PFA) fixed thick bone sections and frozen bone samples.

Keywords

Confocal, two-photon microscopy, cancer metastasis, bone

Introduction

Confocal and two-photon microscopy have been widely used to visualise and track biological events, from the cellular to the molecular level, with the main advantage being able to produce 3D images of thick sample specimens. This provides exciting possibilities to study cellular interactions and microstructures when imaging optically dense tissue such as bone.

The first confocal microscope was developed by Marvin Minsky in 1955 [1] and was widely applied in biological research after its commercial availability in early 1980s [2]. In a confocal microscope, the laser beam is focused by the objective lens into a focal volume within a fluorescent specimen. All emitted fluorescent light from the focal plane will be recollected by the objective lens, focused at the confocal pinhole and passed to the detector, whilst fluorescent light emitted from objects not in focal plane (out-of-focus signal) will hit the edge of the pinhole and be physically blocked from reaching the detector. Therefore, sharper images with better contrast and higher resolution could be achieved using a confocal microscope, compared to the commonly used wide-field fluorescence microscope (Figure 1A). Since the first application in studying human cranial bone microstructure by Alan Boyde in 1990 [3], confocal microscopy has become a powerful tool in research related to the skeletal system, such as assessment of bone microdamage under physiological and pathological conditions [4-6]. Confocal microscopy has also provided opportunities to investigate bone cell-to-cell interactions in three-dimension, which is particular important for research involving osteocytes and osteoblasts [7-11]. More recently using revised and improved bone processing strategy, a significant progress has been made in the imaging of the bone marrow microenvironment and particularly the vasculature in bone. This technical

advance led to the identification of a specialized blood vessel subtype (namely type H) in bone, which forms a niche for osteoprogenitors and thereby regulates bone formation [12-14].

The principle of the two-photon effect was proposed in 1930s by Maria Göppert-Mayer and confirmed in 1961 by Wolfgang Kaiser [15]. During conventional excitation using confocal microscopy, a fluorescent molecule absorbs a single excitation photon with higher energy level and shorter wavelength than emission. For example, a photon of 488nm wavelength is used to excite GFP molecule to emit a 509nm photon. In contrast, in two-photon microscopy, two longer wavelength exciting photons are used to excite the same fluorescent molecule, when these two photons are concentrated or 'fused' in a small volume of specimen (<1 f litre) within a short time period (scale of attoseconds) [16]. In theory, a GFP molecule could be excited by two 976nm photons with half the amount of energy of one 488nm photon [16]. This means the operating wavelength is in the near-infrared range. In addition, as the two-photon effect only occurs at the focal point, the excitation outside the focal plan is limited and hence physically cutting out-of-focus signals with the pinhole is no longer necessary (Figure 1B). All of these offer advantages compared to confocal microscopy, including reduced scattering, enhanced depth penetration, lower phototoxicity, and the ability to excite multiple fluorescent markers with a single excitation wavelength. As bone structures heavily scatter lights and the high collagen content generates second-harmonic signals (SHG), these advantages won two-photon microscopy increasing popularity in research of cellular activities and interactions within bone and marrow, particularly in identifying the haematopoietic stem cell niche and detecting bone metastasis-initiating cancer cells in bone [17-23].

In this article, using the detection of breast cancer cell bone colonisation by confocal and two-photon microscopy as a representative example, we will describe a step-by-step methodology, from sample preparation to data analyses, used to investigate cellular events in frozen and fixed/decalcified mouse bone samples *ex vivo* (See schematic outline, Figure 2). Advantages and limitations of this technology is also discussed to guide the reader as to which is the most appropriate for their research question.

Materials and methods

This methodology, developed for use with the Zeiss LSM510 NLO Upright multiphoton microscope, allows the visualization the 3D structure of frozen/fixed samples of calcified bones and the detection of fluorescent lipophilic dyes labelled cancer cells within the bone marrow, providing essential information on the seeding of cancer cells *in vivo*.

1. Cancer cell preparation and inoculation

On the day of inoculation, breast cancer cells are pre-labelled with fluorescent lipophilic membrane dyes (Vybrant DiD, DiI and CM-DiI, Life Technologies Ltd, Paisley, UK) to facilitate the detection of single cells in the bone microenvironment by multiphoton microscopy. One advantage of using these lipophilic dyes is being able to detect dormant cells as these cell membrane dyes are diluted to nondetectable concentrations in proliferating cells [20-22, 24, 25].

Cancer cells are firstly washed with PBS, trypsinized by 0.15% Trypsin-EDTA for 3-5 minutes, at 37°C at 5% CO_2. Cells are removed with appropriate media containing 10% FBS and centrifuged for 5 minutes at 200g. The cell pellet is re-suspended at a concentration of $1x10^6$ cells/ml in serum free medium for Vybrant DiD labelling or in Hanks' balanced salt solution (HBSS) for Vybrant CM-DiI. Five microliter cell-labeling solution is added per milliliter of cell suspension and incubated at 37°C for 20 minutes (Vybrant DiD) or 5 minutes followed by 15 minutes on ice (Vybrant CM-DiI). Following the incubation, the cell suspension is centrifuged at 200g for 5 minutes. The supernatant is discarded and the cell pellet is re-suspended in PBS. The washing in PBS is repeated three times. Labelled cancer cells are then resuspended at $1x10^5$ cells/mL in PBS for the following intra-cardiac or intra-venous inoculations in immunocompromised mice (100µL/mouse). The cell suspension

should be kept on ice and filtered with 40μm cell strainer prior injection to prevent clumping of cells that could cause an embolism [26].

***Note*:** Unlike DiD and DiI, CM-DiI is a DiI derivative and can be retained in cells throughout fixation, permeabilization and paraffin embedding procedure.

2.1 Frozen bone sample preparation

As previous studies suggested, breast cancer cells locate preferentially in long bones in murine models, tibias and femurs were therefore collected for *ex vivo* two-photon microscopy examination [20, 27]. Other bone samples (e.g. ribs) can also be used for confocal/two-photon microscopy examination but extra care should be taken to maintain consistency of sample orientation while sectioning, which is important for comparison of different samples.

Immediately after animal euthanasia, long bones were dissected free of soft tissue and snap-frozen in liquid nitrogen. The frozen bones were then embedded in Bright Cryo-M-Bed (Bright Instrument Co. Ltd, Huntingdon, UK) and frozen in sample blocks. The embedded tissue blocks are then trimmed longitudinally to expose bone marrow area using a Bright OTF Cryostat with a 3020 microtome (Bright Instrument Co. Ltd, Huntingdon, UK) (Figure 3A). The cutting angle of the blade is set to 22 degrees in order to obtain an even surface crucial to allow optimal imaging of the bone structure. However, the optimal setting of cutting angle could be various depend on different instruments. The bone was placed with the exposed marrow surface inside an uncoated, 35mm glass bottom microwell dish (MatTek Corporation, Ashland, USA) and a coverslip was applied to keep it tightly attaching

to the surface of glass bottom (Figure 3B). Using an upright multiphoton microscope (Zeiss LSM510 NLO, Carl Zeiss Inl, Cambridge, UK) the glass bottom dish has to be placed upside down, with the exposed bone marrow surface facing upwards (Figure 3C). For long scans, ensure to keep the sample moist.

Note: Keeping similar orientations of samples in the blocks is strongly advised. For example, right tibias are placed in blocks with the right fibula facing the right side of the block and the opposite direction is used for the left limb.

2.2 Fixed/decalcified bone sample preparation

Extreme calcification causes opacity and hinders processing of bone tissue preventing its analysis by high-resolution optical imaging. Though extensive and long decalcification steps enable ergonomic tissue handling, these steps mask epitopes of antigens limiting the optimal immunohistochemical analysis. We have recently revised and improved the bone processing strategy, which involves short decalcification, and thick bone sectioning combined with confocal microscopy enables bone imaging at a resolution never achieved before. The methodology provides a novel approach to explore the structural, spatial and morphological components of the bone marrow microenvironment under physiological and pathological conditions. These technical advancements have led to the characterization of distinct vessel subtypes in bone [12-14]. Here, we report this advanced methodology that will provide a platform to close several major knowledge gaps and will therefore greatly facilitate future analyses focusing on the bone marrow. We describe this methodology to acquire high quality images of the bone tissue in a stepwise manner.

In this procedure, freshly isolated bone tissue is fixed immediately using a 4% paraformaldehyde solution for 4 hours at room temperature. The fixed bones are washed in Phosphate Buffered Saline (PBS) and subjected to short decalcification using 0.5M Ethylene Diamine Tetra Acetate (EDTA) solution for 24-48 hours. Decalcified bones are washed thoroughly in PBS and incubated in cryoprotectant solution (20% sucrose and 2% Polyvinyl Pyrrolidone) for 24 hours. Following cryoprotection, bones are suspended in gelatin based embedding solution for 30minutes before being embedded and kept in an ultrafreezer for freezing. The embedding solution composed of 8% gelatin, 20% sucrose and 2% PVP works better than OCT in this protocol. The frozen samples are cut using a cryotome to get tissue sections of appropriate thickness. These cryosections can be further used for immunohistochemical studies to understand the bone marrow microenvironment. The comprehensive methodology from collecting fresh bone tissues to cryosectioning and immunostaining has been described previously [28].

3. Imaging bone samples with confocal/two-photon microscopy

Basic microscope settings

The bone structure can be visualised by second harmonic generation using a Chameleon laser at 900nm (Coherent, Santa Clara, CA.), while Vybrant-DiD labelled cancer cells can be visualised using a 633nm HeNe laser and Vybrant DiI/CM-DiI with a 543nm HeNe laser. The configuration settings and beam paths for different channels are shown in Figure 4A. The second-harmonic generation is detected with BP390-465 (blue, pseudocoloured white in

image Figure 4B), Vybrant-DiI/CM-DiI with BP 565–615 (orange/red, pseudocoloured pink in image Figure 4B) and Vybrant-DiD with BP 650–710 (far red, pseudocoloured red in image Figure 4B).

Note: As multiphoton microscopy has the ability to excite multiple fluorescent markers with a single excitation wavelength, two-photon excitation can be set at 820 nm and multiple fluorescence can be detected using the following: BP435-485 to detect blue (SHG), BP 500–550 to detect green (GFP), and BP 650–710 to detect far-red (DiD) [23]. However, this will increase the energy level of photon and hence higher risk of photobleaching.

Note: Multiphoton work has potential hazard to the eyes depending on laser light wavelength and beam intensity. Damage to the retina can be caused by light within the wavelength range of 400-1400nm, therefore safety goggles must be worn at all times during the procedure.

Visualisation of the specimen with transmitted light

Ensuring that the specimen is flat against the glass bottom dish is crucial for obtaining high quality image of the specimen. Transmitted light is used to visualise the specimen prior to the scanning with the multiphoton laser, via ensuring even focus at all extremities of the specimen and clear vision of both borders of the growth plate.

Setting up the Z-stack

Once the focus on the specimen has been set using transmitted light, visualise the tissue with the Chameleon laser set at 900nm. Adjust the focus up and down until the bone disappears from view to set a temporary upper and bottom boundaries, using the continuous scan function. Move the focal plane to the middle between the two boundaries

and set as zero level where the bone should appear brightest. In the Z-stack setting panel (see note), reset the upper and bottom boundaries depending on the desired depth of the Z-stack scan. For a Z-stack in depth of 70µm, upper and bottom boundaries are set at 35 µm above and below the focal plane (zero level) respectively, with 2µm interval between each scan levels.

Note: The depth of a z-stack should be determined by the weakest laser used in the protocol. At 100% power, the 543nm HeNe laser (for DiI/CM-DiI) could typically achieve acceptable image quality at depth of 70µm, while 633nm HeNe laser (for DiD) could reach 100µm, when used for imaging bone specimens. Although two-photon excitation can in theory image at depths up to 1mm [29], good quality image of bone structure can only be achieved up to 130µm with SHG and the Chameleon laser at 900nm.

Setting up a tile scan

Once satisfied with the z stack setting, move the position beacon to the middle of the specimen. A tile of 5x6 mosaics (an area of 2104µm x 2525µm) is required to cover the growth plate and the metaphysis region of a tibia. It is recommended to check the four corner of the tile to determine if the z-stack boundaries are appropriate for the entire bone, adjusting the z settings if necessary. Reposition the beacon to the middle of the tile and focus at zero plane. The other lasers can then be switched on and a low resolution test tile scan could be run to check the settings and presence of tumour cells in the bone.

Note: It is strongly recommended to use low resolution scanning and maximal scanning speed during the set up stage, i.e. using a frame size of 256 and a mean pixels depth of 1, to quicken this procedure and reduce the potential of photobleaching. Although two-photon

microscopy has the general advantage of reduced photobleaching, high-order photobleaching is still observed within the focal volume [29].

Imaging the bone

To achieve high quality image within the shortest time period, change the frame size to 512, mean pixel depth to 4 and use the maximum speed of scanning (Figure 5A). Prior to the beginning of the scan, correct settings and detailed configuration should be loaded in a Multi Time Series (MTS) software. These include database to store temporary files and the reconstructed tile z-stack image, configuration of laser settings, depth and pixels of the scan, z-stack and tile location. Principal steps and settings of MTS software are shown in Figure 5B. Typically, a scan of 2104µm x 2525µm for 70µm depth using two lasers will take approximately 3 hours and 30 minutes, while using 3 lasers will take up to 6 hours depending on the instrument.

4. Image analysis using Volocity 3D Image Analysis Software

Analysis of the 3D reconstructed, tile z-stack scans can be performed using a range of different software packages, such as the commercially available Volocity 3D Image Analysis (PerkinElmer, Cambridge, UK) or the freely downloadable ImageJ (https://imagej.nih.gov/ij/).

In this methodology, we use Volocity 3D Image Analysis Software to carry out 3D analysis of the scanned tibias. Under the '3D Opacity' mode, the software could be used to provide qualitative data via applying pseudocolour (i.e. white colour for calcified bone tissue by SHG) and adjusting brightness and contrast for different channels (Figure 6A). Under 'extended focus' model, the software could provide quantitative data, i.e. quantifying objectives and

measuring distances between objectives. Upon setting up the quantification protocol, the function 'Find object' was used to identify bone and tumour cells. Objectives detected with 900nm multiphoton laser with a minimum size of 500 μm^3 were considered as bone, while objectives detected by the 633nm HeNe laser with a minimum size of 250 μm^3 and intensity threshold between 90 and 255 were considered Vybrant-DiD labelled breast cancer cells (Figure 6B & 6C). Objectives were quantified within a defined region of interest (ROI) and their distance to the nearest bone surface and to the nearest tumour cell was calculated using the 'Measure distance' option of the software, in addition to the default measurements such as size and signal intensity of the objectives (Figure 6D). Finally, all the quantitative data can be exported as comma-separated values (CSV) file for further statistical analysis.

Discussion

In this manuscript, we have described step-by-step protocols to be used in confocal and two-photon microscopy in cancer bone metastasis research using mouse models.

This method holds a number of advantages over other available techniques for bone imaging. These advantages include: 1. The method generates high-resolution 3D image of the bone microenvironment to understand the spatial and temporal arrangement of multiple cell types within the bone tissue. 2. The thick tissue sections maintain intact structure and cellular morphology, which is essential to understand phenotypic changes in bone structure in genetic studies. 3. The high quality reproducible images generated using this protocol can be used for quantification studies as the method shows low levels of background while maintaining optimal tissue and cellular morphology.

In addition to the techniques related to confocal and two-photon microscopy, good fluorescent labelling techniques are equally important for high quality imaging. It is important to choose the right labelling dyes appropriate to the nature of samples and equipment of laser sources. A panel of the most commonly used fluorescent markers for bone research using confocal and two-photon microscopy are listed in table 1. This will facilitate the readers to decide the choice in usage of confocal or two-photon microscopy, together with considering beneficial factors such as lower photontoxicity and multi-fluorescence excitation by two-photon microscopy. However, deeper penetration depth by two-photon, widely accepted as 6-fold deeper than confocal microscopy using the same sample and fluorophores [29], will not be achieved in thick bone specimens due to their dense nature. In our practice, penetration depth below 150μm by two-photon laser and SHG could

provide optimal images for bone structure, which is not significantly superior to the maximum depth (~100μm) that confocal microscopy could achieve.

Although the methodology is highly advantageous, it has to be used in combination with other advanced techniques such as micro-CT, PET etc to better understand the bone structure. The limitations associated with using this procedure are: 1. This procedure does not provide dynamic data, which limits our understanding of dynamic processes in bone. Although intravital imaging is achieved in cranium, live imaging more dynamic endochondral skeletons is still a milestone need to be achieved [30]. 2. The procedure is unsuitable for quantifying secretory or chemokines in bone. 3. As the procedure involves imaging of thick tissue sections, it is necessary to analyze serial sections and number of samples to verify the phenotypic changes in bone structure. 4. The procedure costs are higher than other techniques due to the high purchase costs of appropriate laser sources and high running costs for longer scanning time.

In conclusion, confocal/two-photon microscopy is a powerful research tool for studying cellular interactions and microstructures in murine bone models. Understanding working principle, background, advantages and limitations of this technique, could help users to adjust and improve their own protocol for applying confocal/two-photon microscopy to cancer bone metastasis research, using our methodology as a reference.

Acknowledgement

We thank Professor Ingunn Holen and Ms Anne Fowles for critical reading of this manuscript and insightful scientific discussion.

Conflict of Interest

All authors state that they have no conflicts of interest.

References:

1. Minsky M. Memoir on Inventing the Confocal Scanning Microscope. Scanning. 1988;10:128-38.

2. Lee K, Yeung H. Application of Laser Scanning Confocal Microscopy in Musculoskeletal Research. In: Qin L, Genant HK, Griffith JF, Leung KS, editors. Advanced Bioimaging Technologies in Assessment of the Quality of Bone and Scaffold Materials. Berlin: Springer Berlin Heidelberg; 2007. p. 173-89.

3. Boyde A, Hendel P, Hendel R, Maconnachie E, Jones SJ. Human cranial bone structure and the healing of cranial bone grafts: a study using backscattered electron imaging and confocal microscopy. Anatomy and embryology. 1990;181(3):235-51.

4. Fazzalari NL, Forwood MR, Manthey BA, Smith K, Kolesik P. Three-dimensional confocal images of microdamage in cancellous bone. Bone. 1998;23(4):373-8.

5. O'Brien FJ, Taylor D, Dickson GR, Lee TC. Visualisation of three-dimensional microcracks in compact bone. Journal of anatomy. 2000;197 Pt 3:413-20.

6. Zarrinkalam KH, Kuliwaba JS, Martin RB, Wallwork MA, Fazzalari NL. New insights into the propagation of fatigue damage in cortical bone using confocal microscopy and chelating fluorochromes. European journal of morphology. 2005;42(1-2):81-90.

7. Kamioka H, Honjo T, Takano-Yamamoto T. A three-dimensional distribution of osteocyte processes revealed by the combination of confocal laser scanning microscopy and differential interference contrast microscopy. Bone. 2001;28(2):145-9.

8. Nesbitt SA, Horton MA. Fluorescence imaging of bone-resorbing osteoclasts by confocal microscopy. Methods in molecular medicine. 2003;80:259-81.

9. Ramires PA, Giuffrida A, Milella E. Three-dimensional reconstruction of confocal laser microscopy images to study the behaviour of osteoblastic cells grown on biomaterials. Biomaterials. 2002;23(2):397-406.

10. Sugawara Y, Kamioka H, Honjo T, Tezuka K, Takano-Yamamoto T. Three-dimensional reconstruction of chick calvarial osteocytes and their cell processes using confocal microscopy. Bone. 2005;36(5):877-83.

11. Akkiraju H, Bonor J, Nohe A. An Improved Immunostaining and Imaging Methodology to Determine Cell and Protein Distributions within the Bone Environment. The journal of histochemistry and cytochemistry : official journal of the Histochemistry Society. 2016;64(3):168-78.

12. Kusumbe AP, Ramasamy SK, Adams RH. Coupling of angiogenesis and osteogenesis by a specific vessel subtype in bone. Nature. 2014;507(7492):323-8.

13. Ramasamy SK, Kusumbe AP, Wang L, Adams RH. Endothelial Notch activity promotes angiogenesis and osteogenesis in bone. Nature. 2014;507(7492):376-80.

14. Kusumbe AP, Ramasamy SK, Itkin T, Mae MA, Langen UH, Betsholtz C, et al. Age-dependent modulation of vascular niches for haematopoietic stem cells. Nature. 2016;532(7599):380-4.

15. Kaiser W, Garrett CGB. Two-Photon Excitation in CaF_2:Eu^{2+}. Physical Review Letters. 1961;7(6):229-31.

16. Kawakami N, Flugel A. Knocking at the brain's door: intravital two-photon imaging of autoreactive T cell interactions with CNS structures. Seminars in immunopathology. 2010;32(3):275-87.

17. Malide D, Metais JY, Dunbar CE. Dynamic clonal analysis of murine hematopoietic stem and progenitor cells marked by 5 fluorescent proteins using confocal and multiphoton microscopy. Blood. 2012;120(26):e105-16.

18. Sano H, Kikuta J, Furuya M, Kondo N, Endo N, Ishii M. Intravital bone imaging by two-photon excitation microscopy to identify osteocytic osteolysis in vivo. Bone. 2015;74:134-9.

19. Xie Y, Yin T, Wiegraebe W, He XC, Miller D, Stark D, et al. Detection of functional haematopoietic stem cell niche using real-time imaging. Nature. 2009;457(7225):97-101.

20. Wang N, Docherty FE, Brown HK, Reeves KJ, Fowles AC, Ottewell PD, et al. Prostate cancer cells preferentially home to osteoblast-rich areas in the early stages of bone metastasis: evidence

from in vivo models. Journal of bone and mineral research : the official journal of the American Society for Bone and Mineral Research. 2014;29(12):2688-96.

21. Wang N, Reeves KJ, Brown HK, Fowles AC, Docherty FE, Ottewell PD, et al. The frequency of osteolytic bone metastasis is determined by conditions of the soil, not the number of seeds; evidence from in vivo models of breast and prostate cancer. Journal of experimental & clinical cancer research : CR. 2015;34:124.

22. Wang N, Docherty F, Brown HK, Reeves K, Fowles A, Lawson M, et al. Mitotic quiescence, but not unique "stemness," marks the phenotype of bone metastasis-initiating cells in prostate cancer. FASEB journal : official publication of the Federation of American Societies for Experimental Biology. 2015;29(8):3141-50.

23. Lawson MA, McDonald MM, Kovacic N, Hua Khoo W, Terry RL, Down J, et al. Osteoclasts control reactivation of dormant myeloma cells by remodelling the endosteal niche. Nature communications. 2015;6:8983.

24. Price TT, Burness ML, Sivan A, Warner MJ, Cheng R, Lee CH, et al. Dormant breast cancer micrometastases reside in specific bone marrow niches that regulate their transit to and from bone. Science translational medicine. 2016;8(340):340ra73.

25. Pece S, Tosoni D, Confalonieri S, Mazzarol G, Vecchi M, Ronzoni S, et al. Biological and molecular heterogeneity of breast cancers correlates with their cancer stem cell content. Cell. 2010;140(1):62-73.

26. Dai J, Hensel J, Wang N, Kruithof-de Julio M, Shiozawa Y. Mouse models for studying prostate cancer bone metastasis. BoneKEy reports. 2016;5:777.

27. Ottewell PD, Wang N, Brown HK, Reeves KJ, Fowles CA, Croucher PI, et al. Zoledronic acid has differential antitumor activity in the pre- and postmenopausal bone microenvironment in vivo. Clinical cancer research : an official journal of the American Association for Cancer Research. 2014;20(11):2922-32.

28. Kusumbe AP, Ramasamy SK, Starsichova A, Adams RH. Sample preparation for high-resolution 3D confocal imaging of mouse skeletal tissue. Nature protocols. 2015;10(12):1904-14.

29. Ustione A, Piston DW. A simple introduction to multiphoton microscopy. Journal of microscopy. 2011;243(3):221-6.

30. Turcotte R, Alt C, Mortensen LJ, Lin CP. Characterization of multiphoton microscopy in the bone marrow following intravital laser osteotomy. Biomedical optics express. 2014;5(10):3578-88.

Titles and legends to figures

Figure 1. Working principle of confocal and multiphoton microscopy. **(A)** In a confocal microscope, all emitted fluorescent light from the focal plane focused at the confocal pinhole and passed to the detector, whilst out-of-focus signal will hit the edge of the pinhole and be physically blocked from reaching the detector. **(B)** In two-photon microscopy, the two-photon effect only occurs at the focal point, therefore out-of-focus signal is limited and no pinhole is needed.

Figure 2. Schematic outline. The step-by-step methodology will be described in details in steps of cancer cell preparation, bone specimen preparation (frozen and fixed sample respectively), confocal/two-photon microscopy imaging, and image analysis.

Figure 3. Preparation of the specimen. **(A)** Long bones should be collected snap frozen and embedded in Bright Cryo-M-Bed and bone marrow exposed a Bright OTF Cryostat with a 3020 microtome. **(B)** The specimen is placed in a glass bottom dish with the exposed marrow surface facing downwards on the dish, specimen need to be hold in place with a coverslip, as shown in real and schematic. **(C)** Using an upright microscope the dish previously prepared should be placed facing upwards and onto a microscopy slide which hold it in place, as shown in real and schematic.

Figure 4. Configuration settings to scan bone and tumour cells labelled with Vybrant-CM-DiI and Vybrant-DiD. Beam paths for the different channels are shown in **(A)**. Mouse tibia scan

in which breast cancer cells labelled with Vybrant-CM-DiI (yellow arrows) and Vybrant-DiD (green arrows) are visible.

Figure 5. Control panel and example of Multi Time Series (MTS) software. The optimal settings are shown in **(A)** while **(B)** is an example of MTS software and a summary of the crucial steps for its setting prior the scan of the specimen.

Figure 6. Image analysis using Volocity 3D Image Analysis Software. **(A)** A 3D reconstruction image of tibia specimen after pseudocolour applied (white colour for calcified bone tissue by SHG) and brightness/contrast adjusted, under the '3D Opacity' mode. **(B)** Under the 'extended focus' model, region of interest (ROI) can be selected with a free hand tool. **(C)** The function 'Find object' was used to identify bone and tumour cells. The settings for identifying tumour cells labelled with DiD are objectives with a minimum size of 250 μm^3 and intensity threshold between 90 and 255. **(D)** Distance from identified tumour cells to the nearest bone surface and to the nearest tumour cell can also be calculated, using the 'Measure distance' option.

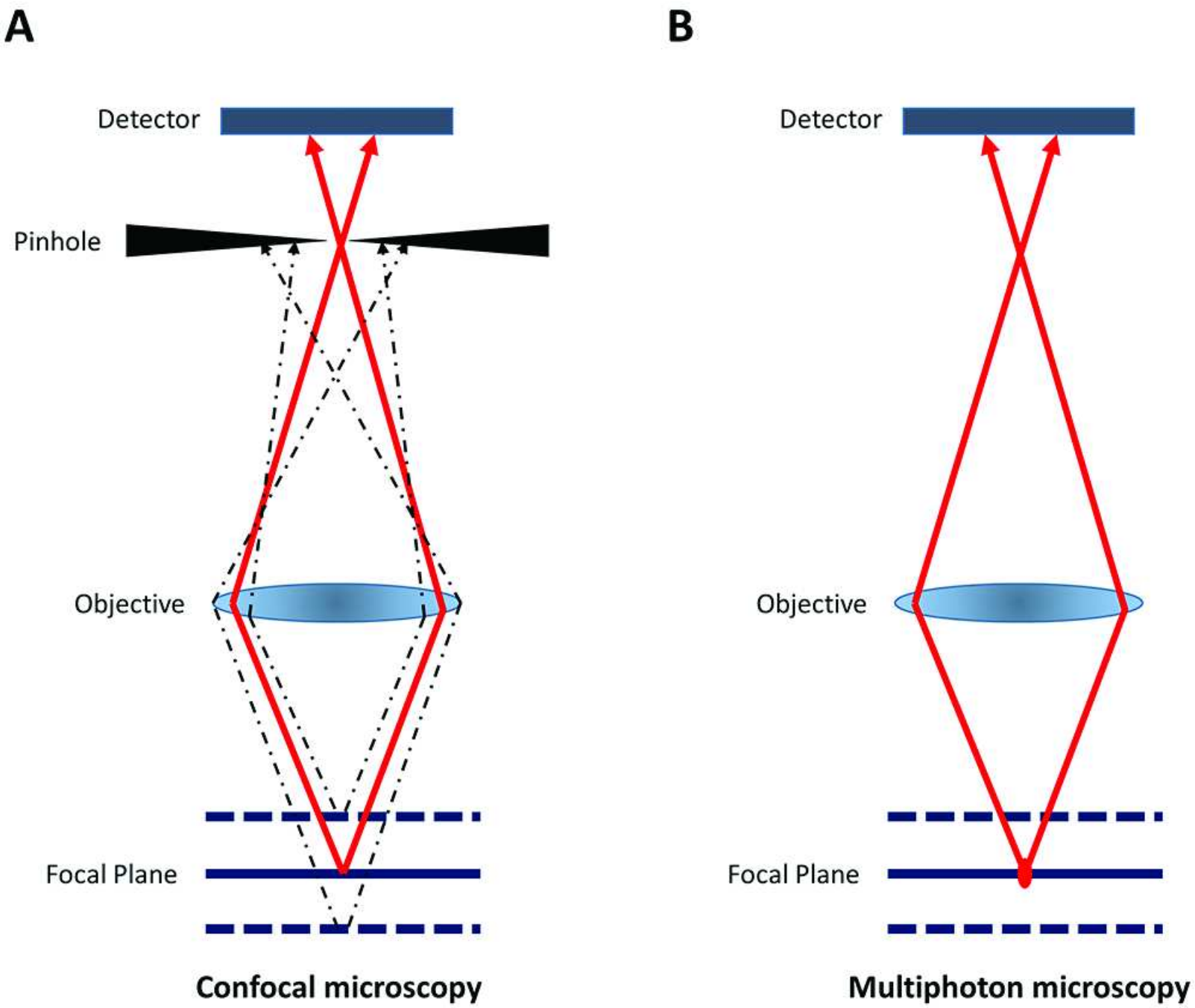
A
Detector
Pinhole
Objective
Focal Plane
Confocal microscopy
B
Detector
Objective
Focal Plane
Multiphoton microscopy

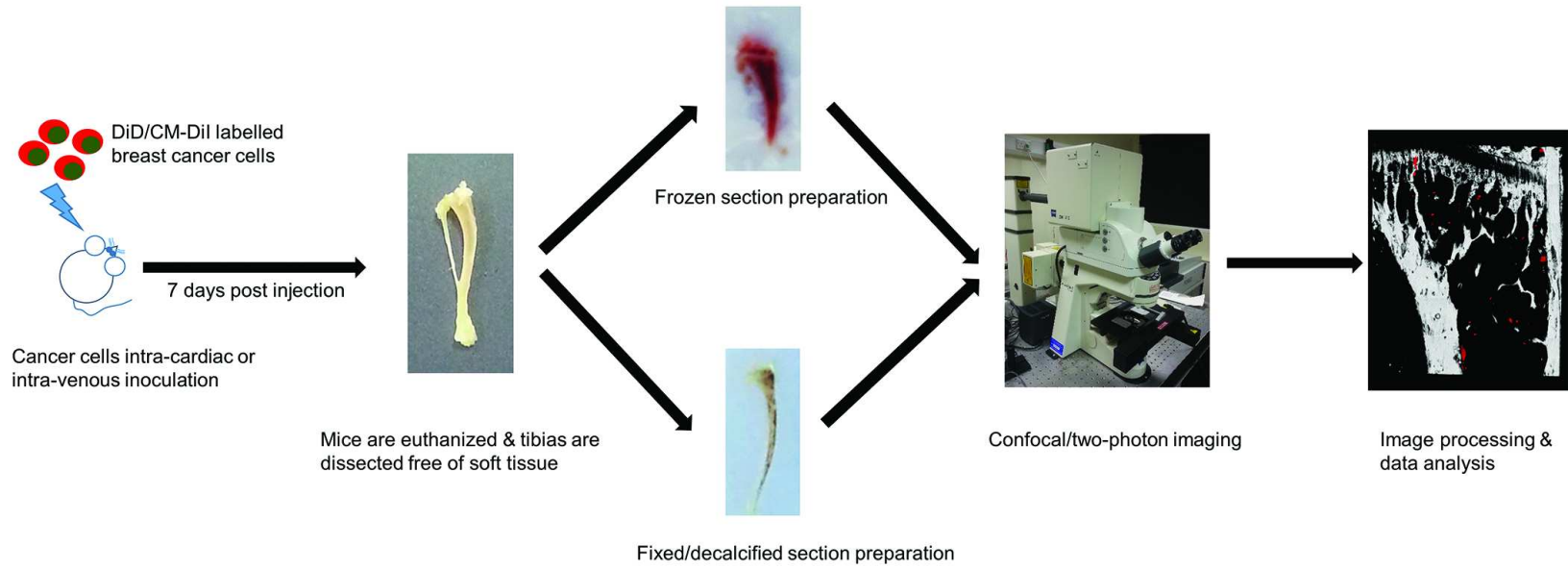
DiD/CM-DiI labelled
breast cancer cells
7 days post injection
Cancer cells intra-cardiac or
intra-venous inoculation
Mice are euthanized & tibias are
dissected free of soft tissue
Frozen section preparation
Fixed/decalcified section preparation
Confocal/two-photon imaging
Image processing &
data analysis

A

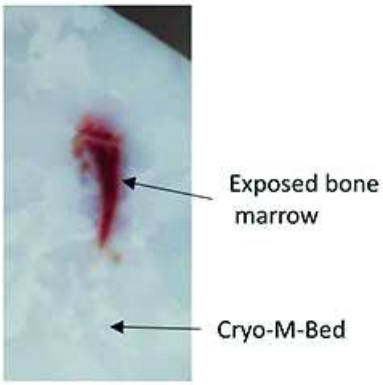
Exposed bone marrow
Cryo-M-Bed

B

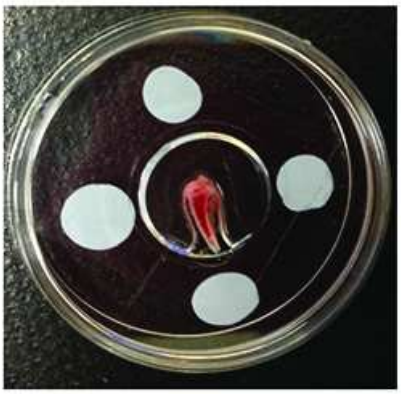

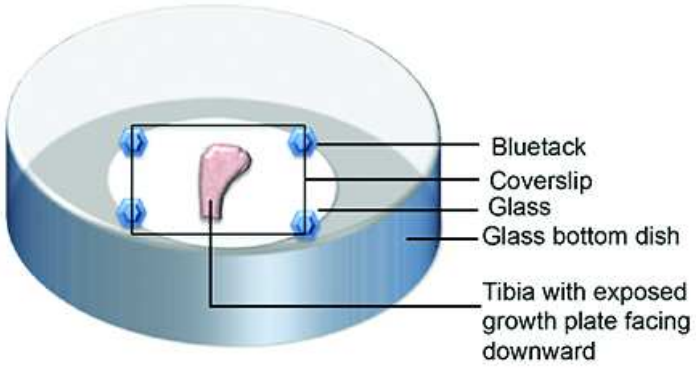
Bluetack
Coverslip
Glass
Glass bottom dish
Tibia with exposed growth plate facing downward

C

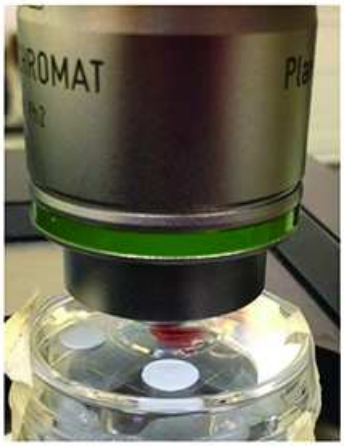
ROMAT

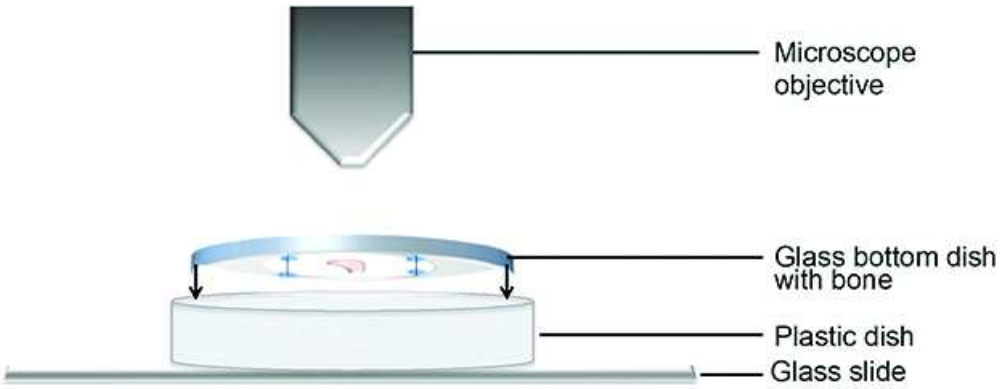
Microscope objective
Glass bottom dish with bone
Plastic dish
Glass slide

A

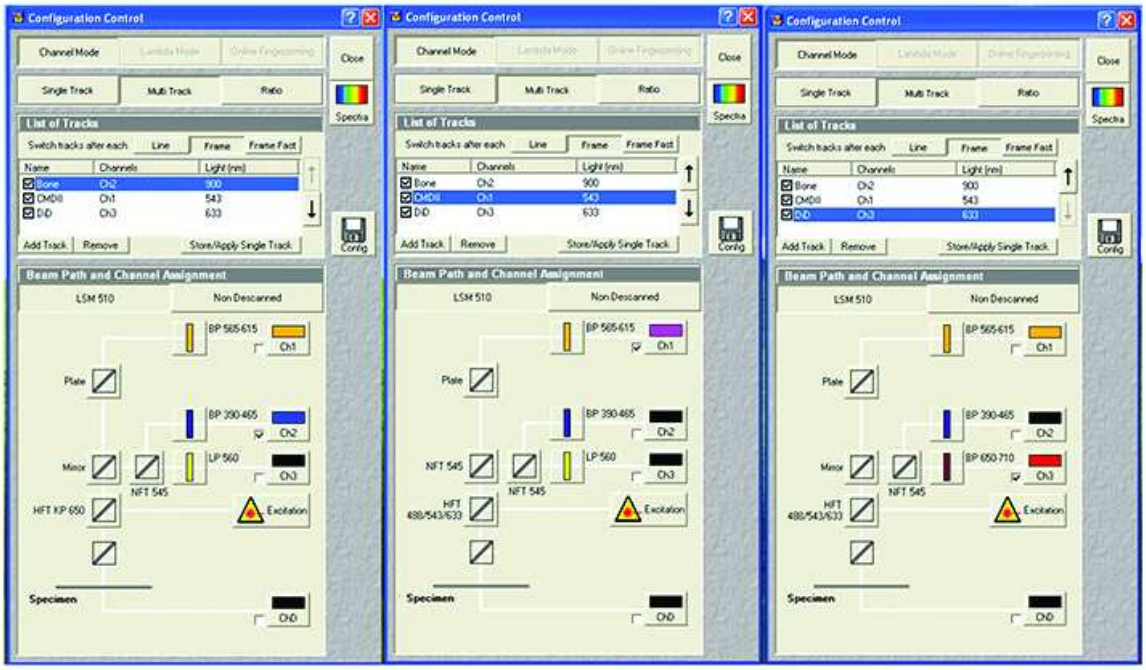
Configuration Control
Channel Mode
Close
Single Track
Multi Track
Ratio
Spectra
List of Tracks
Switch tracks after each
Line
Frame
Frame Fast
Name
Channels
Light (nm)
Bone
Ch2
900
OMDII
Ch1
543
DD
Ch3
633
Add Track
Remove
Store/Apply Single Track
Config
Beam Path and Channel Assignment
LSM 510
Non Descanned
BP 565-615
Ch1
Plate
BP 390-465
Ch2
Mirror
LP 560
Ch3
NFT 545
HFT KP 650
HFT 488/543/633
Excitation
Specimen
Ch0

B

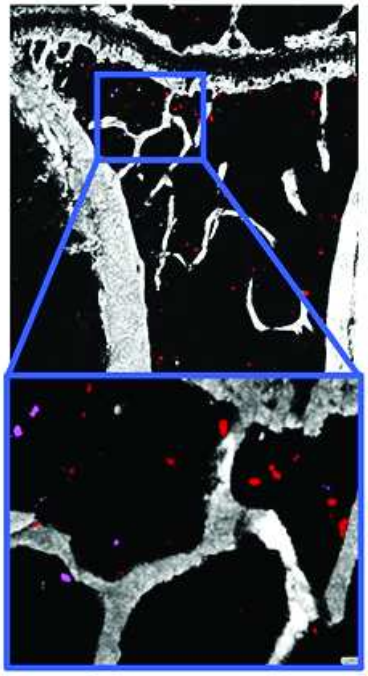

A

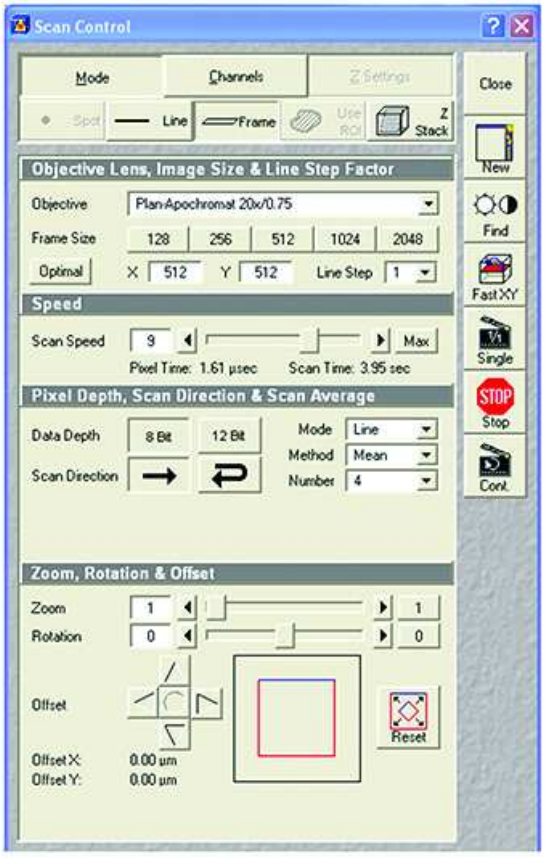

B

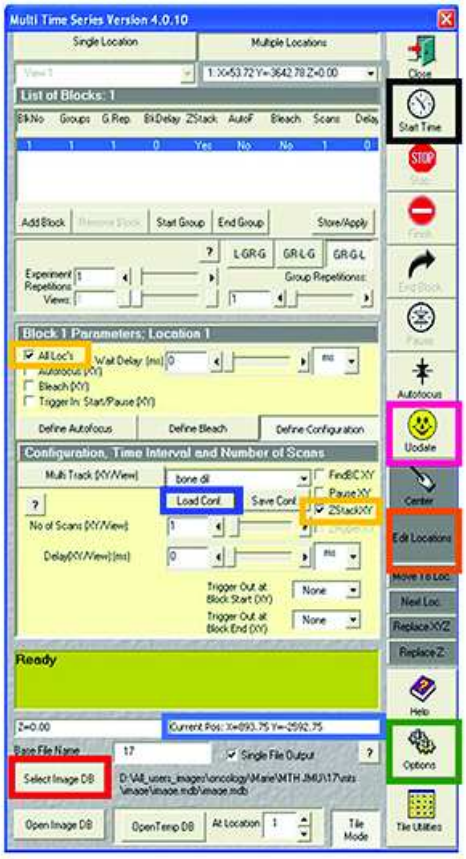

1. Select the image database where to save the reconstructed image
2. Select the temporary database

1. Load the configuration previously saved
2. Edit location and create a tile of 5x6

1. Check that the current position matches with your setting
2. Check that 30 locations are loaded
3. 'All locations' and 'ZstackXY' have to be selected
4. Update
5. Start

A

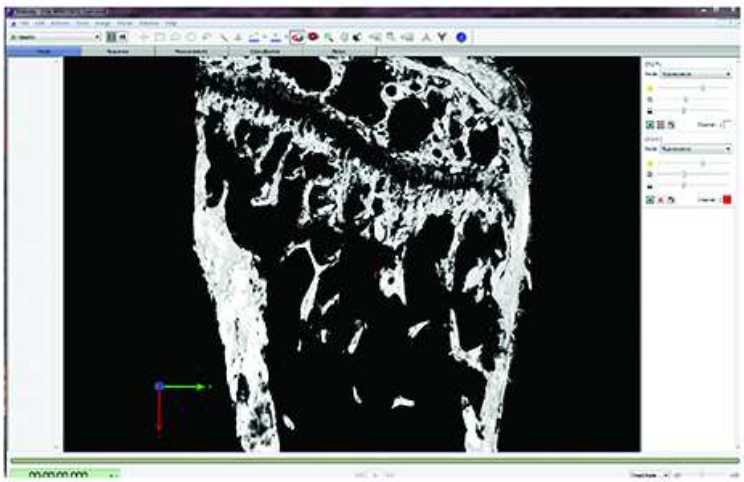

B

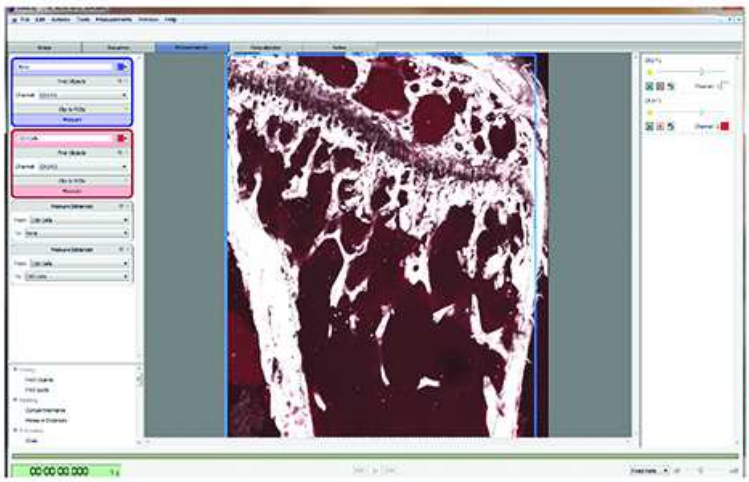

C

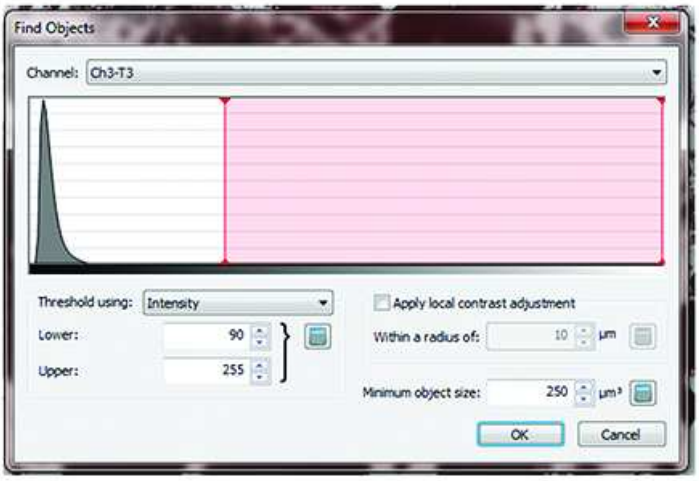
Find Objects
Channel: Ch3-T3
Threshold using: Intensity
Lower: 90
Upper: 255
Apply local contrast adjustment
Within a radius of: 10 µm
Minimum object size: 250 µm³
OK
Cancel

D

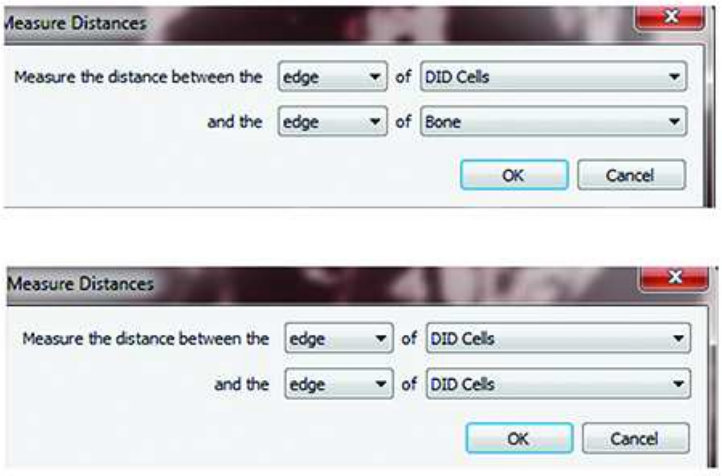
Measure Distances
Measure the distance between the edge of DID Cells
and the edge of Bone
OK
Cancel
Measure Distances
Measure the distance between the edge of DID Cells
and the edge of DID Cells
OK
Cancel

Table 1. Spectra of commonly used fluorescent markers for bone research using confocal and two-photon microscopy

	Two-photon excitation (nm)	**Confocal excitation (nm)**	**Emission (nm)**
eBFP	780	380	440
eCFP	860-920	433	475
eGFP	880-930	488	509
tdTomato	900-1000	554	581
DsRed	930-990	557	592
mCherry	900-1000	587	610
FITC	780-800	494	520
Texas Red	780-920	595	615
Hoechst	780	350	461
DAPI	700	358	461
DiI	700	549	565
DiD	780-820	644	665
DiO	780-830	484	501
Alizarin complexone	900	530-560	580
Calcein	780-900	495	515
Tetracycline	800	390	550
Bone collagen (SHG)	820-900	N/A	450